*Journal of Organometallic Chemistry*, 429 (1992) 119–134
Elsevier Sequoia S.A., Lausanne
JOM 22424

# Spectroscopic investigations of catalytic iridium carbonyl species in sodium chloroaluminate melts

Louis J. Tortorelli [a], Paul A. Flowers [a], Brisco L. Harward [a], Gleb Mamantov [a] and Leon N. Klatt [b]

[a] *Department of Chemistry, University of Tennessee, Knoxville, TN 37996-1600 (USA)*
[b] *Analytical Chemistry Division, Oak Ridge National Laboratory, Oak Ridge, TN 37831-6142 (USA)*

(Received May 28, 1991)

**Abstract**

*In situ* spectroscopic studies of the iridium chemistry occurring during the catalytic hydrogenation of carbon monoxide employing $IrCl(CO)_3$ and $Ir_4(CO)_{12}$ in an aluminum chloride-sodium chloride (63:37 mole%) melt were performed. Infrared, UV-visible, Raman, and $^1H$ NMR data indicate that similar monomeric species are generated during catalysis. Infrared investigation of the introduction of $IrCl(CO)_3$ into molten $AlCl_3$:NaCl (63:37) under $CO:H_2$ (1:3 mole ratio) and the reaction between $IrCl(CO)_3$ and carbon monoxide in an acidic melt suggest the initial formation of an iridium-carbonyl species followed by the generation of a hydridocarbonyl complex in the initial stage of the catalysis. Infrared data also indicate that the method of introduction for $Ir_4(CO)_{12}$ into the $AlCl_3$:NaCl medium under 1 atm of $CO:H_2$ (1:3 mole ratio) has a marked effect on the spectra observed. In an acidic melt $IrCl(CO)_3$ reacts with hydrogen to form hydrogen chloride, methane and metallic iridium.

## Introduction

The threat of low oil and natural gas reserves in the early 1970's initiated extensive investigations of hydrocarbon production via the reduction of carbon monoxide by hydrogen, i.e. the Fischer–Tropsch reaction. The Fischer–Tropsch process traditionally involves the use of heterogeneous catalysts [1–4] and yields straight-chain hydrocarbons along with alkenes and oxygenated compounds as primary products.

Interest in homogeneous Fischer–Tropsch catalysis has been stimulated in part by the potential for increased product selectivity [5,6] and milder reaction conditions [7]. For example, Thomas *et al.* [7] have observed the reduction of carbon monoxide to methane utilizing $Os_3(CO)_{12}$ and $Ir_4(CO)_{12}$ as the homogeneous catalyst precursors in organic solvents at 140°C and approximately 2 atm of

Correspondence to: Dr. G. Mamantov, Department of Chemistry, University of Tennessee, Knoxville, TN 37996-1600, USA.

pressure; unfortunately, slow reaction rates were observed. The authors also noted that "classic" mononuclear complexes, under identical reaction conditions, were catalytically inactive. Hydrogenation of carbon monoxide using soluble mononuclear complexes as catalysts has been demonstrated [8,9], but temperatures above 200°C and pressures between 200 and 1300 atm were required, and only oxygenated products were produced.

Investigations of chemical systems in molten salt media often show that the solvent plays an active role in the solute chemistry. This is frequently the case for chloroaluminate melts (mixtures of aluminum chloride with other chloride salts) where the Lewis acidity may be adjusted by varying the aluminum chloride concentration [10]. Chloroaluminate melts are termed acidic, neutral, or basic if the mole ratio of aluminum chloride to companion salt is greater than, equal to, or less than one, respectively.

Demitras and Muetterties [11] first reported on the catalytic activity of $Ir_4(CO)_{12}$ under $CO:H_2$ (1–2 atm) in an acidic sodium chloroaluminate melt (160–180°C). In a subsequent study, Muetterties and coworkers [12] performed a more detailed analysis of this system, including infrared analysis of frozen catalyst-melt reaction mixtures obtained in Nujol mulls. For reaction times in excess of one hour, bands were observed at 2190, 2160, 2125, 2112, and 1630 $cm^{-1}$ for the resultant iridium carbonyl species. Without the $CO:H_2$ fill gas, $Ir_4(CO)_{12}$ decomposed as evidenced by the disappearance of all bands in the carbonyl stretching region.

Collman *et al.* [13] conducted a kinetic study of the same catalytic system under flow and recycle conditions, and also demonstrated that $IrCl(CO)_3$ is active as a catalyst precursor. Different product distributions from those of Muetterties and coworkers [11,12] were obtained in this work, and it was concluded that a different active catalyst was produced. Although no spectra were shown, it was stated that a multiband pattern was observed in the 2000–2200 $cm^{-1}$ region.

The major difference between the procedures employed by the two groups was the method of introduction of $Ir_4(CO)_{12}$ into the melt. Muetterties and coworkers premixed the iridium complex with the frozen melt before heating (pre-melt addition), whereas Collman *et al.* added the iridium complex to the melt at 175°C (post-melt addition).

There are two interesting and potentially advantageous traits of this chloroaluminate melt-based catalytic system, namely (1) the melt apparently serves as a promoter allowing carbon monoxide reduction to occur at relatively low pressures and temperatures, and (2) oxygenated products are not generated. Presented herein are the results of *in situ* spectroscopic studies of molten sodium chloroaluminate solutions of $IrCl(CO)_3$ and $Ir_4(CO)_{12}$ under various atmospheres conducted with the hope of identifying the catalytically active species present in this chemical system. A preliminary account of this work has appeared in the Proceedings of a Symposium [14].

## Experimental

*Reagents.* Dodecacarbonyltetrairidium, $Ir_4(CO)_{12}$, and chlorotricarbonyliridium(I), $[IrCl(CO)_3]_n$, were purchased from Strem Chemicals Inc. and used without further purification. Prepurified nitrogen (99.998%, MG Scientific Gases), high-

purity carbon monoxide (99.8%, Air Products), hydrogen (99.9%, Air Products), and deuterium (99% Linde Specialty Gases) were used as received. Tetramethylammonium bromide (TMAB) was obtained from Fluka Chemical and recrystallized from methanol three times. Anhydrous aluminum chloride (> 99%, Fluka Chemical) was purified by an extraction/distillation procedure similar to one described previously [15]. Sodium chloride (reagent grade, Mallinckrodt, Inc.) was vacuum-dried at 400°C for four days before use. The sodium chloroaluminate melts were prepared by fusing the appropriate quantities of aluminum chloride and sodium chloride in an evacuated sealed pyrex ampule at 175°C.

*Instrumentation.* Infrared spectra were acquired with a Digilab FTS-20E Fourier transform infrared spectrometer (Bio-Rad, Digilab Division) operating at an instrumental resolution of 4 $cm^{-1}$. The IR cell employed for all *in situ* measurements has been described previously [16]. Gas-phase IR spectra were obtained in a vacuum-tight cell equipped with KBr windows. Raman spectra were acquired using a Jobin–Yvon Ramanor 2000M spectrometer equipped with an Instruments S.A. Inc. Model 980015 controller and a Pacific Model 126 photometer. The argon-ion laser line at 514.5 nm from a Spectra Physics Model 171 laser was used to illuminate the sample. UV-visible spectra were recorded with a rapid-scanning spectrometer (RSS) system [17]. Raman and UV-visible cells were constructed from Pyrex and quartz according to previously reported designs [18]. Proton nuclear magnetic resonance spectra were recorded on JEOL FX90Q spectrometer operating at 89.55 MHz with tetramethylammonium bromide (TMAB) as the internal reference set to 3.21 ppm. All NMR spectra were obtained with the spectrometer operating on external lock. X-Ray photoelectron spectra were acquired with the Perkin-Elmer PHI 5100 ESCA System.

*Procedure.* Due to the moisture and air sensitivity of aluminum chloride, all manipulations involving melts were performed in a Vacuum Atmospheres glove box (moisture level < 2 ppm) with prepurified nitrogen as the filler gas. Reagent gases were added to the sample cells either prior to melting via a vacuum manifold (the pressure was measured at this point) or afterwards from a sealed Pyrex tube equipped with a break seal. Likewise, the iridium carbonyls were introduced to the chloroaluminate salts either prior to melting by simply mixing the two solids or afterwards by means of a FLICKET valve assembly (Ace Glass, Inc.).

## Results

*Spectra under nitrogen.* A solution of $IrCl(CO)_3$ in a 63 mole percent (m/o) $AlCl_3$ melt at 175°C under 1 atm of nitrogen results in a clear yellow solution whose infrared spectrum exhibits the bands listed in Table 1. In a 49 m/o melt a significantly different infrared spectrum was observed; the observed bands are also listed in Table 1.

Previous investigations [12,13] have shown that $Ir_4(CO)_{12}$ is unstable in acidic sodium chloroaluminate melts in the absence of a significant pressure (> 0.1 atm) of carbon monoxide; under these conditions the cluster decarbonylates as evidenced by carbon monoxide evolution and precipitation of iridium metal [11].

For comparison purposes, the relevant infrared bands of $IrCl(CO)_3$ and $Ir_4(CO)_{12}$ in KBr pellets and of pure $IrCl(CO)_3$ studied by diffuse reflectance are also listed in Tables 1 and 2, respectively.

Table 1

CO stretching frequencies obtained from the IR spectra of $IrCl(CO)_3$

| $IrCl(CO)_3$ | $\nu$(CO), $cm^{-1}$ [a] |
|---|---|
| Pure solid (spectrum obtained by diffuse reflectance) | 2143(m), 2132(s), 2100(s), 2090(s) 2050(s), 2025(m) |
| KBr | 2143(m), 2132(s), 2100(s), 2090(s), 2059(s), 2024(m) |
| $AlCl_3$:NaCl (63:37)-$N_2$ | 2178(m), 2168(w), 2143(m), 2125(s) 2107(m), 2085(w) |
| $AlCl_3$:NaCl (49:51)-$N_2$ | 2170(w), 2153(w), 2126(w), 2087(s) 1985(s) |
| $AlCl_3$:NaCl (63:37)-CO | 2125(s) |
| $AlCl_3$:NaCl (63:37)-CO:$H_2$ (pre-melt addition) | 2230(w), 2187(m), 2157(s), 2125(m) |
| $AlCl_3$:NaCl (63:37)-CO:$D_2$ (pre-melt addition) | 2187(m), 2176(sh), 2157(s), 2125(m) |
| $AlCl_3$:NaCl (63:37)-CO:$H_2$ (post-melt addition) $t = 0$ h | 2187(vw), 2178(vw), 2157(vw), 2168(vw), 2125(s), 2085(vw) |
| $AlCl_3$:NaCl (63:37)-$H_2$ | 2125, 2107 (decay) 2178, 2168, 2157, 2143 (growth-decay) 2075(w), 2041(w) (growth) |

[a] s = strong, m = medium, w = weak, sh = shoulder.

*Spectra under carbon monoxide.* Infrared spectra of $IrCl(CO)_3$ in a 63 m/o melt under 1 atm of carbon monoxide at 150°C exhibit a single intense band at 2125 $cm^{-1}$. The intensity of this band remained constant over the 24 h period examined, indicating the presence of a stable iridium species. The infrared spectrum of $IrCl(CO)_3$ in a 49 m/o melt under 1 atm carbon monoxide was similar to that obtained under nitrogen.

The initial infrared spectrum of $Ir_4(CO)_{12}$ in a 63 m/o melt under 1 atm of carbon monoxide at 150°C exhibited bands at the frequencies listed in Table 2. After 3–4 h, the band at 2143 $cm^{-1}$ disappeared and the intensity of the band at 2125 $cm^{-1}$ increased. There were no differences in the infrared spectra obtained if the solution was stirred manually or if it was quiescent.

Solutions of $IrCl(CO)_3$ and $Ir_4(CO)_{12}$ in a 63 m/o melt under 1 atm of carbon monoxide at 150°C yielded similar UV-visible spectra with maxima at 278, 326, and 430 nm. The intensity of these bands increased with time; however, the rate of growth was slower for $Ir_4(CO)_{12}$. After 10 h the ratio of the molar absorptivities of these bands for the solutions of the cluster and the monomer was 4:1, indicating that the iridium cluster reacted to form a mononuclear complex. The rate of this

Table 2

CO stretching frequencies obtained from the IR spectra of $Ir_4(CO)_{12}$

| $Ir_4(CO)_{12}$ | $\nu$(CO), $cm^{-1}$ [a] | | |
|---|---|---|---|
| KBr | 2112(w), 2090(wsh), 2056(s), 2023(m), 2006(wsh) | | |
| $AlCl_3$:NaCl (63:37)-CO, $t = 0$ h | 2157(w), 2143(s), 2125(m), 2107(sh), 2083(w) | | |
| $AlCl_3$:NaCl (63:37)-CO, $t = 4$ h | 2156(w), 2125(s), 2110(sh), 2083(w) | | |
| $AlCl_3$:NaCl | $t = 1$ h | $t = 10$ h | $t = 24$ h |
| (63:37)-CO:$H_2$ (Pre-melt addition) | 2187(m) | 2187(m) | 2187(w) |
| | | | 2178(s) |
| | | | 2168(sh) |
| | 2157(s) | 2157(s) | 2157(m) |
| | | | 2143(s) |
| | | | 2132(m) |
| | 2125(m) | 2125(m) | |
| | | 2114(m) | |
| | 2107(m) | 2107(sh) | 2107(w) |
| | 2085(w) | | |
| | | 1656(w) | 1656(m) |
| $AlCl_3$:NaCl-CO:$D_2$ | $t = 1$ h | $t = 10$ h | $t = 24$ h |
| (63:37) | | | 2182(s) |
| (Pre-melt addition) | 2176(w) | 2178(m) | |
| | | 2168(vw) | 2168(w) |
| | 2157(m) | 2157(s) | |
| | | | 2143(s) |
| | 2125(s) | 2131(s) | 2125(m) |
| | 2107(s) | 2107(m) | 2107(m) |
| | 2085(m) | | |
| | | 1639(w) | 1639(m) |
| $AlCl_3$:NaCl-(63:37) CO:$H_2$, $t = 0$ h (Post-melt addition) | 2164(sh), 2157(w), 2140(s), 2134(s), 2125(s), 2105(m), 2085(sh), 2043(vw) | | |
| $AlCl_3$:NaCl-(63:37) CO:$H_2$, $t = 4$ h (Post-melt addition) | 2187(sh), 2180(m), 2170(sh), 2154(m) 2143(m), 2125(s), 2107(s), 2085(m), 2043(w) | | |
| $AlCl_3$:NaCl-(63:37) CO:$H_2$, $t = 9$ h (Post-melt addition) | 2230(w), 2187(m), 2157(s), 2125(m) | | |

[a] s = strong, m = medium, w = weak, vw = very weak, sh = shoulder.

conversion was shown to follow first-order kinetics. An average rate constant of $1.32 \pm 0.26 \times 10^{-4}$ $s^{-1}$ was calculated from the data obtained using the three UV-visible bands.

Raman spectra of $Ir_4(CO)_{12}$ in a 63 m/o melt (post-melt addition) under 1 atm carbon monoxide at 150°C exhibited a weak band at 202 $cm^{-1}$, which disappeared within one hour after introduction of the cluster to the melt. This band is within the region expected for a metal–metal stretch [19], and its dependence upon the

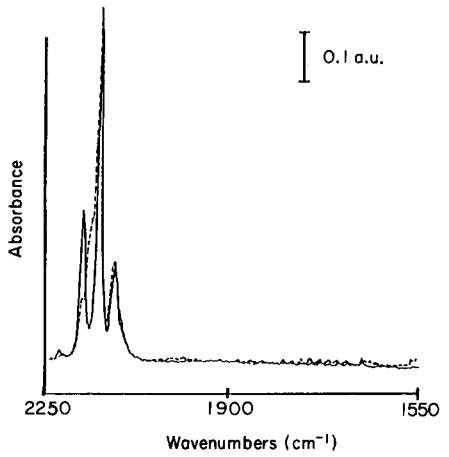


Fig. 1. Infrared spectra of $IrCl(CO)_3$ in 63 m/o $AlCl_3$ melts under 1 atm of $CO:H_2$ (solid curve) and $CO:D_2$ (dashed curve); $[IrCl(CO)_3] = 8$ m$M$, 175°C. Mole ratio of $CO_{gas}$ to $IrCl(CO)_3 > 4$.

polarization state of the exciting radiation suggests that it is a symmetric vibration. Under identical conditions, this band was not observed with $IrCl(CO)_3$.

*Spectra under carbon monoxide:hydrogen.* A solution of $IrCl(CO)_3$ (pre-melt addition) in a 63 m/o melt under 1 atm $CO:H_2$ (1:3 mole ratio) was clear and yellow in color. The infrared spectrum, shown in Fig. 1, exhibited bands at the frequencies listed in Table 1. The intensities of these infrared bands were essentially constant over the 24 h period examined. This behavior was also observed upon addition of $CO:H_2$ to a solution containing $IrCl(CO)_3$ initially under a carbon monoxide atmosphere.

The infrared spectrum observed immediately after the addition of $IrCl(CO)_3$ (post-melt addition) to a 63 m/o melt under 1 atm of $CO:H_2$ at 170°C exhibited the bands listed in Table 1. Between 2.5 and 6 h the intensity of the band at 2125 $cm^{-1}$ decreased while the intensity of the bands at 2187 and 2157 $cm^{-1}$ increased. After 6 h the intensities of these bands remained essentially constant. Five days later the intensity of the 2125 $cm^{-1}$ band decreased while the 2187 and 2157 $cm^{-1}$ bands increased.

A solution of $Ir_4(CO)_{12}$ (pre-melt addition) in a 63 m/o melt under 1 atm of $CO:H_2$ (1:3 mole ratio) at 175°C is clear and yellow in color. The infrared spectrum of a 2 m$M$ solution, shown in Fig. 2, exhibited bands, listed in Table 2, whose relative intensities changed over the course of a 24 h period, indicating the presence of several iridium carbonyl species of different stabilities. About 1 h after melting, bands were observed at 2187, 2157, 2125, 2107 and 2085 $cm^{-1}$. At 10 h the intensities of the 2187 and 2157 $cm^{-1}$ bands increased considerably relative to the other bands while the intensities of the 2107 and 2085 $cm^{-1}$ bands decreased; a very weak band was observed at 1656 $cm^{-1}$. After 24 h the intensities of the 2187 and 2157 $cm^{-1}$ bands started to decrease, the 1656 $cm^{-1}$ band grew substantially, and new and intense features were observed at 2178 and 2143 $cm^{-1}$.

The dynamic behavior of $Ir_4(CO)_{12}$ is illustrated in Fig. 3, which shows the variation in the observed absorbance for several of the prominent spectral features

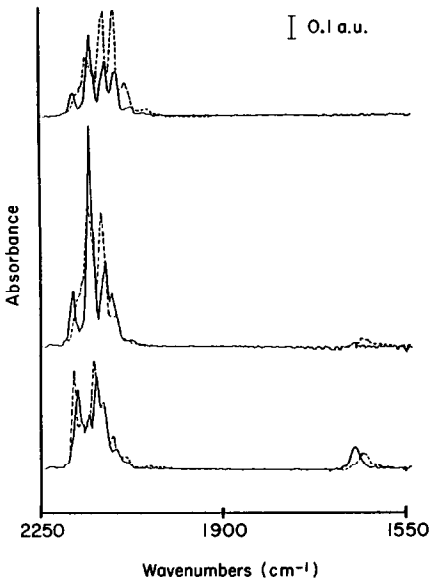


Fig. 2. Infrared spectra of $Ir_4(CO)_{12}$ in 63 m/o $AlCl_3$ melts (pre-melt addition) under 1 atm of $CO:H_2$ (solid curve) and $CO:D_2$ (dashed curve) obtained *ca.* 1 h (upper), 10 h (middle), and 24 h (lower) after melting; $[Ir_4(CO)_{12}] = 2$ m*M*, 175°C.

as a function of time. Essentially three different responses are observed, i.e., decay (2125, 2107 and 2085 $cm^{-1}$ bands), growth (2178, 2143, and 1656 $cm^{-1}$ bands), and growth followed by decay (2187 and 2157 $cm^{-1}$ bands). For an 8 m*M* solution of $Ir_4(CO)_{12}$ the intensities of the 2125, 2107 and 2085 $cm^{-1}$ bands steadily increased until reaching a maximum value at about 18 h; the 1656 $cm^{-1}$ band appeared only as a weak transient feature, disappearing entirely by the end of the 24 h period examined.

When $Ir_4(CO)_{12}$ is added to a 63 m/o melt at 170°C (post-melt addition) under 1 atm of $CO:H_2$ (1:3 mole ratio), different dynamics of the infrared spectral features were observed. The bands observed as a function of time are listed in Table 2. After about 9 h, bands at 2230, 2187, 2157 and 2125 $cm^{-1}$ were observed. The last spectrum, taken after 41 hours, was very similar to the spectrum shown in Fig. 1.

An interesting result from the infrared studies was the observed growth of melt oxide bands [20], *i.e.*, solvated AlOCl, at 791 and 691 $cm^{-1}$ as a function of time. Figure 4 shows the increase in absorbance for the 791 $cm^{-1}$ band for the solutions containing $IrCl(CO)_3$ and $Ir_4(CO)_{12}$. These results support previous reports [12,13] that the melt serves as an oxide "sink" during the course of the reaction, consuming any intermediate oxygenated products (including water) via reaction with $AlCl_3$. Figure 4 also points to a slower rate of catalysis exhibited by the monomer relative to the cluster species; this behavior has been previously reported [13].

In the UV-visible spectral region solutions of $IrCl(CO)_3$ in 63 m/o melt under 1 atm of $CO:H_2$ exhibited absorption maxima at 272, 322, 406, and 430 nm, which

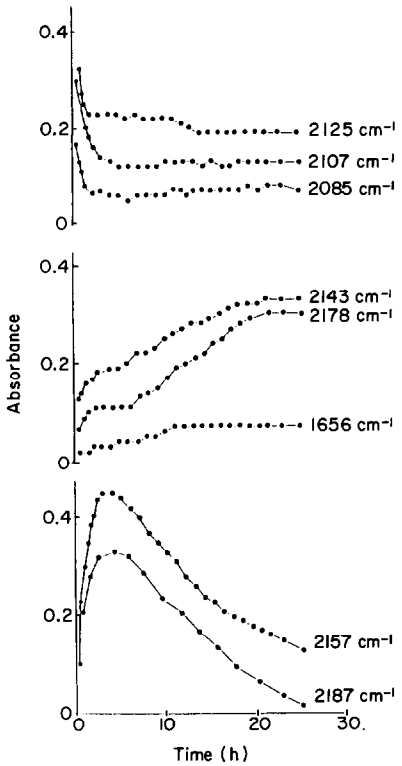


Fig. 3. Plots of absorbance versus time after melting for several prominent features from the spectra for the $CO:H_2$ system shown in Fig. 2.

increased in intensity as a function of time. The short wavelength region (< 250 nm) was characterized by a rapidly increasing absorption. The position and relative intensities of the bands at 272, 322, and 430 nm were very similar to the spectrum

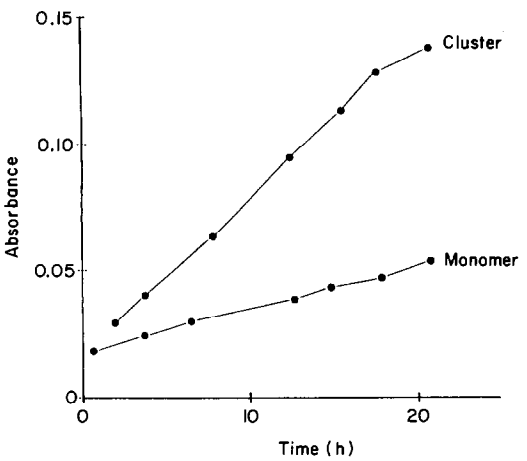


Fig. 4. Plots of absorbance at 791 $cm^{-1}$ *versus* time after melting for 2 m*M* $Ir_4(CO)_{12}$ (upper curve) and 8 m*M* $IrCl(CO)_3$ (lower curve) in 63 m/o $AlCl_3$ melts under 1 atm $CO:H_2$.

obtained under carbon monoxide. Under identical conditions, similar results were obtained for solutions of $Ir_4(CO)_{12}$.

The Raman spectrum of $Ir_4(CO)_{12}$ in 63 m/o melt (post-melt addition) under 1 atm of $CO:H_2$ (1:3 mole ratio) at 150°C showed the same weak, transient band at 202 $cm^{-1}$ as was observed under a carbon monoxide atmosphere. Again, this band was absent from the spectrum of $IrCl(CO)_3$ under identical conditions.

$^1H$ NMR spectra of $IrCl(CO)_3$ (pre-melt addition) in a 63 m/o melt under 1 atm of $CO:H_2$ (1:3 mole ratio) at 130°C exhibited one major peak at −10.7 ppm *vs.* TMAB (internal reference, 3.21 ppm *vs.* TMS [21]) over the 36 h time period examined; this feature was observed immediately after melting. Two much weaker proton resonances at −19.5 (0.9% the intensity of the peak at −10.7 ppm) and +5.4 ppm (1.3% the intensity of the peak at −10.7 ppm) appeared about 2 h after melting. No significant change in the intensity of these resonances was observed throughout the experiment.

$^1H$ NMR spectra of $Ir_4(CO)_{12}$ in a 63 m/o melt (pre-melt addition) under 1 atm of $CO:H_2$ at 130°C exhibited a major resonance at −10.7 ppm, which appeared roughly 1.5 h after melting and remained throughout the 24 h period the reaction was monitored. Weaker proton resonances were observed at −19.5 and +1.4 ppm. The peak at +1.4 ppm, first observed about 3 h after melting, was initially flanked by two other resonances at +0.9 and +0.3 ppm which disappeared after 4 h. The relative intensities of the two weaker features at −19.5 and +1.4 ppm increased roughly twofold during the 24 h reaction period. Toward the end of the experiment a proton resonance appeared at +5.3 ppm (28% the intensity of the peak at −10.7 ppm). When the $^1H$ NMR spectra of $Ir_4(CO)_{12}$ were acquired with TMAB as an external reference, an additional peak at +3.6 ppm was observed about 5 h after melting. Spectral interference from the TMAB prevented the observation of this resonance when TMAB was used as an internal reference. During the course of the experiment, the intensity of the resonance at +3.6 ppm increased while the intensity of the major resonance at −10.7 ppm decreased.

A $^1H$ NMR spectrum of a 63 m/o $AlCl_3$ melt under hydrogen chloride atmosphere at 130°C exhibited a proton resonance at +1.6 ppm.

*Spectra under carbon monoxide: deuterium.* As the catalytically active species in Fischer-Tropsch systems are frequently hydridocarbonyl complexes, the experiments performed under $CO:H_2$ were repeated under $CO:D_2$. Such isotopic substitution has long been employed in the study of transition metal hydridocarbonyl species [22].

A solution of $IrCl(CO)_3$ (pre-melt addition) under 1 atm of $CO:D_2$ (1:3 mole ratio) yielded an infrared spectrum which remained unchanged for the 24 h period examined (see Table 1 and Fig. 1). A solution of $Ir_4(CO)_{12}$ under similar conditions exhibited transient behavior similar to that observed under $CO:H_2$ (see Table 2 and Fig. 2). Frequency shifts relative to the hydrogen systems were observed for some of the carbonyl bands in each of the mixtures, suggesting that the species produced under the employed conditions are hydrido- (or deuterido-) carbonyls. Such frequency shifts are a result of resonance interaction between the C–O and Ir–H vibrational states.

*Reaction of $IrCl(CO)_3$ with hydrogen.* The reaction of $IrCl(CO)_3$ with hydrogen in a 63 m/o melt at 175°C was also studied. After introduction of hydrogen to a solution initially under nitrogen, the infrared spectra exhibited a decay of bands at

2125 and 2107 $cm^{-1}$, growth followed by the decay of bands at 2178, 2168, and 2143 $cm^{-1}$, appearance of two weak bands at 2075 and 2041 $cm^{-1}$, and a new band at 2157 $cm^{-1}$ which appeared upon introduction of the hydrogen and then totally decayed. The infrared spectra also revealed the growth of melt oxide bands at 691 and 791 $cm^{-1}$ as the reaction proceeded. During the course of the reaction, the solution changed color from a clear, bright yellow to cloudy gray. Upon termination of the reaction, denoted by the formation of the cloudy gray solution, a bright silvery substance formed on the glass walls of the reaction vessel. X-Ray photoelectron spectroscopic analysis revealed this precipitate to be metallic iridium. Infrared analysis of the gas phase above the reaction mixture showed the presence of hydrogen chloride and methane.

## Discussion

*Spectra under nitrogen.* The increase in the carbonyl stretching frequencies observed for $IrCl(CO)_3$ in an $AlCl_3$:NaCl melt under a nitrogen atmosphere relative to those observed for the pure solid or in KBr (see Table 1) indicates a reduction in the amount of electron density at the iridium metal center. This reduced electron density results in decreased back-bonding between the iridium and the $\pi^*$ orbitals of the carbonyl ligand, hence a stronger C–O bond and a higher stretching frequency. This reduction in electron density at the metal center could result from an increase in the oxidation state of iridium and/or the formation of a Lewis acid adduct with aluminum chloride. Adduct formation could occur at the chloride ligand, the oxygen atoms of the carbonyl ligands, or the iridium atom itself [23]. Adducts in which the aluminum atom of aluminum chloride coordinates directly to the metal center of a carbonyl complex typically result in increases of 65–125 $cm^{-1}$ in the carbonyl stretching frequencies, while adducts involving coordination through the chloride ligand generally show increases of about 20 $cm^{-1}$ [23,24]. A Lewis-acid adduct in which the aluminum chloride coordinates to the oxygen atom of a terminal carbonyl ligand has been discarded as a possibility in this case since such adducts exhibit decreases in the stretching frequencies of the complexed carbonyl ligand [23,25].

Thus, the infrared results suggest the formation of a solvated species, $IrCl(CO)_3L_x$ ($L = AlCl_3$), in acidic melts under a nitrogen atmosphere.

*Spectra under carbon monoxide.* As noted earlier, $Ir_4(CO)_{12}$ decomposes to iridium metal in an acidic sodium chloroaluminate melt under an inert atmosphere; however, under a carbon monoxide atmosphere, soluble iridium complexes are generated. Infrared spectra of both the cluster and the monomer in acidic melts under carbon monoxide exhibit a strong terminal carbonyl band at 2125 $cm^{-1}$, suggesting that the same complex is generated from both precursors. This contention is also supported by the UV-visible spectroscopic data. The additional features observed in the infrared spectra of the cluster suggest the formation of at least one other iridium carbonyl complex. The delay in the appearance of the three bands in the UV-visible spectra and in the single major feature in the infrared spectra exhibited by the cluster system indicates that $Ir_4(CO)_{12}$ is experiencing an additional reaction in the melt before generating the final product *i.e.*, fragmentation to a mononuclear complex. Such a reaction is supported by the observed 4:1

ratio of the molar absorptivities for $Ir_4(CO)_{12}$ vs. $IrCl(CO)_3$ obtained from the UV-visible measurements and the transient band at 202 $cm^{-1}$ in the Raman spectrum of the cluster under carbon monoxide.

Possible structures for an iridium-carbonyl complex that exhibits one carbonyl stretching frequency in its infrared spectrum are $Ir(CO)_6^{3+}$, *trans*-$Ir(CO)_4L_2^+$ ($L = AlCl_3$), $Ir(CO)_4^-$, $Ir(CO)_3L_2$ (trigonal bipyramid), and *trans*-$Ir(CO)_2X_2L_2$ [26,27a]. The most likely structure for the iridium complex generated under carbon monoxide, given the spectroscopic data above, is *trans*-$Ir(CO)_4L_2^+$. It is worth noting that $Ru^I$ and $Ir^I$ square planar complexes form similar adducts with boron Lewis acids [27b]. All of the possible iridium-carbonyl complexes containing three or fewer carbonyl ligands are ruled out since such a species should have been generated in the acidic melt under nitrogen. The possibility of forming either $Ir(CO)_6^{3+}$ or $Ir(CO)_4^-$ is likewise discounted since these species would require that the iridium atom undergo a two-electron oxidation or reduction, respectively. Also, the carbonyl stretching frequency for $Ir(CO)_4^-$, reported at 1895 $cm^{-1}$ [28], would be expected to occur at a frequency lower than 2125 $cm^{-1}$ even if a Lewis acid adduct was formed with the solvent. The role of aluminum chloride in the above reaction is evident from the data obtained from an identical reaction performed in a sodium chloride saturated melt. As mentioned in the Results section, no reaction was observed when carbon monoxide was added to a basic melt solution containing $IrCl(CO)_3$ originally under a nitrogen atmosphere.

*Spectra under CO:$H_2$, $D_2$.* In a previous report by Collman *et al.* [13], it was stated that a similar iridium complex is generated from the $IrCl(CO)_3$ and $Ir_4(CO)_{12}$ precursors in the chloroaluminate Fischer–Tropsch system. This has been further substantiated by *in situ* IR, NMR and UV-visible spectroscopy in this work; however, the greater number of peaks observed in the IR (pre-melt addition) and NMR spectra for the cluster relative to the monomer indicate that additional iridium complexes are generated in the cluster system. These additional iridium complexes are generated upon melting when $Ir_4(CO)_{12}$ is premixed with the frozen melt.

The experiments involving the introduction of $IrCl(CO)_3$ to an acidic melt at 170°C under $CO:H_2$ suggest that the carbonyl bands located at 2187, 2157, and 2125 $cm^{-1}$ may be attributed to two different complexes. One complex is responsible for the band at 2125 $cm^{-1}$, which is generated from the reaction between $IrCl(CO)_3$ and carbon monoxide and is the same complex formed under a carbon monoxide atmosphere in the melt. This complex then reacts with hydrogen to generate a complex that exhibits carbonyl bands at 2187 and 2157 $cm^{-1}$.

When $Ir_4(CO)_{12}$ is introduced into the melt at 170°C, it appears that a reaction occurs between the cluster and carbon monoxide and/or hydrogen. This interaction could be responsible for the stoichiometric amount of methane generated in the initial segment of the reaction as observed by Collman *et al.* [13]. The eventual formation of the iridium complexes that give rise to infrared bands at 2187, 2157, and 2125 $cm^{-1}$ supports the claim by Collman *et al.* [13] that similar iridium complexes are generated in the Fischer–Tropsch reaction.

The reaction mixtures under $CO:H_2$ or $CO:D_2$ which utilize $Ir_4(CO)_{12}$ as the catalyst precursor (pre-melt addition) represent complex and dynamic chemical systems as shown by previous reports [12,13] and the data presented here. Based on the observed time dependent responses, at least four different iridium carbonyl

species (one for each type of response) appear to be produced under these conditions (see Fig. 3). For at least two of these species, frequency shifts are observed upon substituting deuterium for hydrogen in the fill gas mixtures, indicating that the complexes produced contain hydride (or deuteride) ligands. In a hydridocarbonyl complex, resonance interaction between the $\nu$(CO) and $\nu$(IrH) vibrational levels may occur if these states are of similar energy and symmetry [29].

The species initially produced from the oxidative fragmentation of $Ir_4(CO)_{12}$ which decays with time exhibited infrared bands at 2125, 2107, and 2085 $cm^{-1}$ under both $CO:H_2$ and $CO:D_2$ gas mixtures (these bands were observed as constant spectral features for solutions of the cluster under carbon monoxide). This complex, termed species **A**, apparently does not contain a hydride (or deuteride) ligand.

Another species, termed **B**, which is also produced from $Ir_4(CO)_{12}$ under $CO:H_2$ and then decays during the 24 h period, gave strong bands at 2187 and 2157 $cm^{-1}$; under $CO:D_2$, this complex exhibited bands at 2176 and 2157 $cm^{-1}$.

Species produced from $Ir_4(CO)_{12}$ under $CO:H_2$ which are gradually generated over the 24 h period examined give rise to bands at 2178, 2143, and 1656 $cm^{-1}$; under $CO:D_2$, these species exhibit bands at 2182, 2143, and 1639 $cm^{-1}$. The curves presented in Fig. 3 suggest that two different carbonyl complexes are produced, one species $\mathbf{C_1}$, represented by the two higher frequency bands and the other, species $\mathbf{C_2}$, by the low frequency band (*i.e.*, at 10 h, the intensity of the 1656 $cm^{-1}$ feature had stabilized; both 2178 and 2143 $cm^{-1}$ bands increased continually over the 24 h period). Since no bands were observed to shift from the 1900–2200 $cm^{-1}$ region to the 1300–1600 $cm^{-1}$ region upon substituting deuterium for hydrogen [29], no Ir–H or Ir–D bands could be assigned. Failure to observe metal hydride or deuteride infrared bands is a fairly common occurrence [29,30]. The shifts in the carbonyl stretching frequencies upon deuteration, however, offer indirect evidence that the species do contain hydride (or deuteride) ligands. More direct evidence for the existence of hydridocarbonyl species is obtained from the $^1H$ NMR spectra (see below). The low-frequency IR bands at 1656 and 1639 $cm^{-1}$ exhibited by $Ir_4(CO)_{12}$ under $CO:H_2$ and $CO:D_2$, respectively, suggest that a polynuclear iridium complex is formed since carbonyl frequencies in this region are characteristic of bridging carbonyl-Lewis acid adducts [31]. The shift which occurs upon deuteration in this case is a result of resonance interaction between the $\nu$(IrD) and the bridging $\nu$(CO) levels. Although no bands were observed in the C–H stretching region (2800–3200 $cm^{-1}$), the possibility that these low frequency (*ca.* 1650 $cm^{-1}$) features are due to carbonyl stretching of a formyl group produced by insertion of carbon monoxide between the metal and a hydride (or deuteride) ligand cannot be excluded [13].

The major spectral changes resulting from deuterium substitution in the $IrCl(CO)_3$ system were the decrease in relative intensity of the highest frequency band at 2187 $cm^{-1}$ and the appearance of a shoulder on the 2157 $cm^{-1}$ band at about 2176 $cm^{-1}$ (Fig. 1). This may likewise be interpreted as a shift of one of two closely placed features around 2187 to 2176 $cm^{-1}$; this is the same behavior as observed for the cluster system at 10 h (pre-melt addition). The presence of additional bands observed for the cluster system (*e.g.*, at 2114 $cm^{-1}$), indicates the formation of additional carbonyl species upon melting when the cluster is pre-mixed with the frozen melt.

The infrared spectra of $Ir_4(CO)_{12}$ solutions (pre-melt addition) under $CO:H_2$ and $CO:D_2$ at long reaction times have several features in common with the spectrum of $IrCl(CO)_3$ under nitrogen. Although the spectra for the cluster system contain additional bands (e.g., the bridging carbonyl features), there appears to be a significant spectral contribution from a species similar to that which results from the monomer under nitrogen, most noticeably at 2143 $cm^{-1}$. This may reflect production of this species from other hydride (or deuteride) complexes as the fill gas is depleted during the course of the reaction. Based on the results of experiments in which $CO:H_2$ was added to solutions initially under nitrogen, it appears that regeneration of the alleged catalyst may be accomplished by simply replenishing the fill gas. In cases where carbon monoxide is the limiting reagent, however, it seems likely that the excess hydrogen will react with the monomeric iridium carbonyl complex in the manner observed for solutions of $IrCl(CO)_3$ under hydrogen, generating methane, hydrogen chloride, and metallic iridium.

By comparison (pre-melt addition experiments), the reaction mixture utilizing $IrCl(CO)_3$ as the catalyst precursor resulted in a much simpler system containing an iridium carbonyl species which was relatively stable over the 24 h period examined. The greater stability of the monomer relative to the cluster system may be due to the relatively higher pressures of reactant gases present in the former system throughout the time period examined. The $CO:H_2$ or $CO:D_2$ pressure is expected to be greater at any given time during the reaction for the monomer system because (a) $Ir_4(CO)_{12}$ rapidly consumes a stoichiometric amount of reactants (*i.e.*, carbon monoxide and hydrogen or deuterium) as it decomposes at the onset of the reaction, and (b) the reaction rate for the $IrCl(CO)_3$ system is about 20% slower than that of the cluster [13]. Thus after 24 h, the cluster system has depleted the fill gas pressure to levels where the catalytic iridium species become unstable; the monomer system, however, has consumed less of the fill gas at this point and is still in the "steady state" regime of reactant concentration. This behavior is illustrated in Fig. 4; the cluster system clearly exhibits a more rapid rate of reaction.

The indirect evidence for the generation of a iridium-hydride complex obtained from the infrared studies is substantiated by the $^1H$ NMR data. The proton resonance at $-10.7$ ppm observed in the $^1H$ NMR spectra of the monomer and cluster suggests that both iridium precursors generate a similar complex in the acidic melt under $CO:H_2$, possibly $HIr(CO)_4(AlCl_3)_x$. The presence of other proton resonances observed for the cluster precursor likewise supports the contention that other hydrogen-containing iridium species are generated (the peak observed at $+1.6$ ppm for a sample of pure melt under a hydrogen chloride atmosphere precludes assignment of any observed proton resonances to dissolved hydrogen chloride). These other major proton resonances observed in the $^1H$ NMR spectra for $Ir_4(CO)_{12}$ are a result of the additional iridium complexes generated when $Ir_4(CO)_{12}$ is premixed with the frozen melt. The other proton resonances may be a result of formyl- or alkyl-Ir protons.

It has been noted that the transient characteristics of infrared spectra for an 8 m*M* solution of $Ir_4(CO)_{12}$ under $CO:H_2$ differed from those of a 2 m*M* solution. This observation suggests that different species (or different relative concentrations of two or more species) are produced from different initial concentrations of $Ir_4(CO)_{12}$. This behavior together with the different results obtained depending on

the method of addition of the iridium complex into the melt is consistent with the observed discrepancies between the works of Collman *et al.* [13] and Muetterties and coworkers [11,12], in which the initial cluster concentrations were about 2 (post-melt addition) and 8 m*M* (pre-melt addition), respectively, and supports the assertion [13] that different catalytic species were produced by the two groups.

## Conclusion

The spectroscopic data reported here show that both iridium complexes generate the same active catalyst when added to the melt and that the method of introduction to the melt has a profound effect on the infrared spectra obtained for the cluster system. As indicated in the Discussion section, the following reaction scheme for $Ir_4(CO)_{12}$ in the presence of carbon monoxide and hydrogen in the acidic melt (pre-melt addition) is proposed.

(a) Rapid oxidative fragmentation of $Ir_4(CO)_{12}$ to yield a complex that has infrared bands at 2125, 2107, and 2085 $cm^{-1}$ (species **A**).

(b) Production and then depletion of a complex with infrared bands at 2187 and 2157 $cm^{-1}$ (species **B**) from species **A**.

(c) Gradual production of two complexes, one with infrared bands at 2178 and 2143 $cm^{-1}$ (species $\mathbf{C}_1$) and the other with a band at 1656 $cm^{-1}$ (species $\mathbf{C}_2$) from species **B**.

By comparison to analogous studies [32], it seems likely that species **B** represents the catalytically active species in this medium. As the reaction proceeds and the fill gas is depleted, this species becomes unstable and is converted to different complexes, species $\mathbf{C}_1$ and $\mathbf{C}_2$. Based upon the observed frequency shifts accompanying deuterium substitution, it appears that species **B**, $\mathbf{C}_1$, and $\mathbf{C}_2$ are all hydridocarbonyl complexes.

It is clear that the $Ir_4(CO)_{12}$ precursor, in the premixed experiments, generates other iridium complexes in addition to those produced from $IrCl(CO)_3$. It also appears that these additional species may exhibit catalytic activity and may be responsible for the discrepancies in the product distribution observed by Muetterties [11] and Collman [13].

The proposed reaction between $IrCl(CO)_3$ and hydrogen in the acidic melt is:

$$2IrCl(CO)_3 + 6AlCl_3 + 19H_2 \rightarrow 2Ir + 6CH_4 + 14HCl + 6AlOCl$$

This reaction presumably is the fate of the iridium carbonyl catalyst at the end of the reaction carried out in the presence of excess hydrogen. When performed under an excess of carbon monoxide, the iridium-carbonyl complex that gives rise to the infrared band at 2125 $cm^{-1}$ is generated at the end of the process. This complex can then regenerate the catalyst when the synthesis gas is reintroduced into the system.

The proposed reaction schemes for the "post-melt addition" for both $IrCl(CO)_3$ and $Ir_4(CO)_{12}$ in an acidic melt under different atmospheres are given below ($L = AlCl_3$):

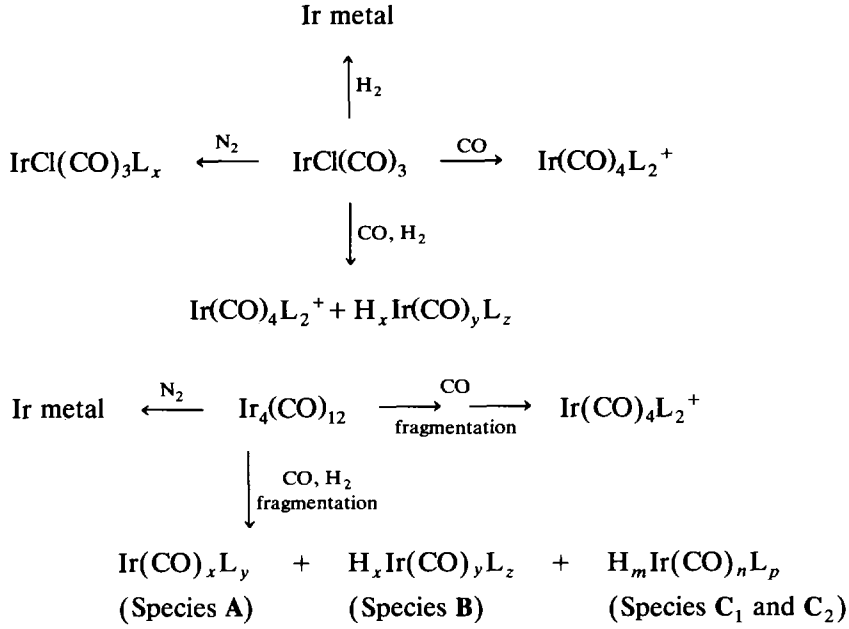


Unambiguous identification of the active catalyst in this system would have been greatly aided if the far infrared region ($< 600$ cm$^{-1}$) had been accessible. Unfortunately, strong solvent absorptions in this region prevented observation of the iridium–ligand vibrations. An attempt was made to use a shorter path length cell which brought the solvent absorptions on scale, but such a short path length prevented observations of the relatively weak metal–ligand bands. Many attempts at isolation of the iridium complexes from the melt were unsuccessful (*e.g.*, distillation and extraction) and indicated these species to be stable only under the employed reaction conditions.

Finally, it should be noted that Collman *et al.* have pointed out the limited technological importance of a catalytic process which consumes aluminum chloride [13]. Nonetheless, the chloroaluminate-based system described herein represents a unique example of the homogeneous Fischer–Tropsch reaction which may serve as a model for more practical catalytic systems. Such systems may include the regeneration of anhydrous aluminum chloride from aluminum oxychloride and related species [33,34].

## Acknowledgements

This work was supported in part by Grants 85-08321 and 88-0307 from the Air Force Office of Scientific Research and in part by the U.S. Department of Energy, Office of Energy Research, under contract DE-AC05-84OR21400 with Martin Marietta Energy Systems, Inc. B.L. Harward acknowledges support from the Laboratory Graduate Participation Program administered by the Oak Ridge Associated Universities for the U.S. Department of Energy. The authors acknowledge D. Trimble for obtaining the Raman spectra, and helpful discussions with G.P. Smith, C.E. Barnes, R.M. Pagni, and C. Woods. We are grateful to a reviewer for helpful suggestions for the interpretation of some of the results.

## References


1 P. Sabatier and J.B. Senderens, C.R. Acad. Sci., 134 (1902) 514.
2 H.H. Storch, N. Golumbic and R.B. Anderson, Fischer Tropsch and Related Synthesis, Wiley, New York, 1951.
3 (a) C.M. Bartish and G.M. Drissel, Kirk-Othmer Encyl. Technol., Wiley, New York, Vol. 4, 3rd ed., 1978, p. 778; (b) G.A. Mills and J.A. Cusumano, *ibid.*, Vol. 5, 3rd ed., 1978, p. 45.
4 G. Henrici-Olive and S. Olive, Angew. Chem., Int. Ed., Engl. 15 (1976) 136.
5 G.N. Schrauzer (ed.), Transition Metals in Homogeneous Catalysis, Marcel Dekker, New York, 1971.
6 J.S. Bradley, J. Am. Chem. Soc., 101 (1979) 7419.
7 M.G. Thomas, B.F. Beier and E.L. Muetterties, J. Am. Chem. Soc., 98 (1976) 1296.
8 J.W. Rathke and H.M. Feder, J. Am. Chem. Soc., 100 (1978) 3623.
9 B.D. Dombek, J. Am. Chem. Soc., 103 (1981) 6508.
10 G. Mamantov and R.A. Osteryoung, in G. Mamantov (Ed.), Characterization of Solutes in Nonaqueous Solvents, Plenum Press, New York, 1978.
11 G.C. Demitras and E.L. Muetterties, J. Am. Chem. Soc., 99 (1977) 2796.
12 H-K. Wang, H.W. Choi and E.L. Muetterties, Inorg. Chem., 20 (1981) 2661.
13 J.P. Collman, J.I. Brauman, G. Tustin and G.S. Wann III, J. Am. Chem. Soc., 105 (1983) 3913.
14 G. Mamantov, L.J. Tortorelli, P.A. Flowers, B.L. Harward, D.S. Trimble, E.M. Hondrogiannis, J.E. Coffield, A.G. Edwards and L.N. Klatt, in C.L. Hussey, S.N. Flengas, J.S. Wilkes and Y. Ito (Eds.), Proceedings of the Seventh International Symposium on Molten Salts, The Electrochemical Society, Inc., Pennington, NJ, 1990, pp. 794–804.
15 R. Marassi, J.Q. Chambers and G. Mamantov, J. Electroanal. Chem., 69 (1976) 345.
16 P.A. Flowers and G. Mamantov, Anal. Chem., 61 (1989) 190.
17 L.N. Klatt, J. Chromatogr. Sci., 17 (1979) 225.
18 V.E. Norvell, G. Mamantov, in D.G. Lovering and R.J. Gale (Eds.), Molten Salt Techniques, Vol. 1, Plenum Press, New York, 1983, Chap. 7.
19 F.A. Cotton and R.A. Walton, Multiple Bonds Between Metal Atoms, John Wiley & Sons, New York, 1982, Chap. 8.
20 P.A. Flowers and G. Mamantov, Anal. Chem., 59 (1987) 1062.
21 Nuclear Magnetic Resonance Spectra, Sadtler Research Laboratories, Inc., Philadelphia, PA, (1966) 6820M.
22 H.D. Kaesz and R.B. Saillant, Chem. Rev., 72 (1972) 231.
23 B.V. Lokshin, E.B. Rusach, Z.P. Valueva, A.G. Ginzburg and N.E. Kolobova, J. Organomet. Chem., 102 (1975) 535.
24 K.D. Karlin, B.F.G. Johnson and J. Lewis, J. Organomet. Chem., 160 (1978) C21; B.F.G. Johnson, K.D. Karlin and J. Lewis, *ibid.*, 174 (1979) C29.
25 S.B. Butts, S.H. Strauss, E.M. Holt, R.E. Stimson, N.W. Alcock and D.F. Shriver, J. Am. Chem. Soc., 102 (1980) 5093.
26 C.M. Lukehart, Fundamental Transition Metal Organometallic Chemistry, Brooks/Cole, Monterey, CA, 1985, p. 80.
27 (a) F.A. Cotton and G. Wilkinson, Advanced Inorganic Chemistry: A Comprehensive Text, 5th ed., John Wiley & Sons, New York, 1988, pp. 901–917; (b) D.F. Shriver, Accounts Chem. Res., 3 (1970) 231.
28 J.L. Vidal and W.E. Walker, Inorg. Chem., 20 (1981) 249.
29 G.L. Geoffroy and J.R. Lehman, Adv. Inorg. Chem. Radiochem., 20 (1977) 190.
30 M.Y. Darensbourg and C.E. Ash, Adv. Organomet. Chem., 27 (1987) 1.
31 (a) A. Alich, N.J. Nelson, D. Strope and D.F. Shriver, Inorg. Chem., 11 (1972) 2976; (b) J.S. Kristoff, D.F. Shriver, *ibid.*, 13 (1974) 499.
32 R. Whyman, J. Organomet. Chem., 94 (1975) 303.
33 (a) C.B. Mamantov, T.M. Laher, R.P. Walton and G. Mamantov, in H.O. Bohner (Ed.), Light Metals 1985, The Metallurgical Society of AIME, 1985, pp. 519–528; (b) G. Mamantov and C.B. Mamantov, U.S. Patent 4, 493, 784, January 15, 1985.
34 I.W. Sun, K.D. Sienerth and G. Mamantov, J. Electrochem. Soc., 138 (1991) 2850.